Journal of Pharmaceutical and Biomedical Analysis 51 (2010) 1047–1053

Contents lists available at ScienceDirect

Journal of Pharmaceutical and Biomedical Analysis

journal homepage: www.elsevier.com/locate/jpba

Study and characterization of crystalline hydrate/polymorph forms of 5,11-dihydro-11-ethyl-5-methyl-8-(2-(1-oxido-4-quinolinyl)ethyl-6H-dipyrido(3,2-B:2′,3′-E)(1,4)diazepin-6-one by solid-state NMR and solution NMR

N.C. Gonnella*, John A. Smoliga, Scot Campbell, Carl A. Busacca, Michael Cerreta[1], Richard Varsolona[2], Daniel L. Norwood

Boehringer Ingelheim Pharmaceuticals Inc., 900 Ridgebury Rd., Ridgefield, CT 06877, United States

ARTICLE INFO

Article history:
Received 8 July 2009
Received in revised form 19 October 2009
Accepted 9 November 2009
Available online 13 November 2009

Keywords:
^{13}C solid-state NMR
Rapid quantitation
Chemical shift assignments
^{1}H relaxation
Degree of crystallinity

ABSTRACT

A novel inhibitor of reverse transcriptase was studied by solid-state NMR. Three phases of the compound were examined which included the dihydrate and two anhydrous polymorphs (Form I and Form III). By correlating ^{1}H and ^{13}C solution NMR with the solid-state ^{13}C NMR CP/MAS and CPPI spectral editing experiments, comparative ^{13}C assignments were made for each phase. Polymorphs of Form I and Form III and the dihydrate were easily distinguished based upon chemical shift patterns of the carbon resonances. The ^{1}H spin-lattice relaxation times were also measured for each phase which provided information on the mobility and relative crystallinity. The ^{13}C ssNMR spectrum of Form I showed the presence of a minor component identified as the dihydrate. Weight/percent quantitation of major and minor components in Form I was obtained from integrated intensities of a 50:50 mixture containing weighed amounts of Form I and the pure dihydrate. Comparison of the ssNMR and X-ray powder diffraction techniques is discussed.

1. Introduction

The enzyme reverse transcriptase (RT) is an essential component of the life cycle of the human immunodeficiency virus type 1 (HIV-1). It is believed that inhibition of the RT viral enzyme should provide an effective means of blocking the spread of HIV-1 infection. Compounds that interfere with the function of the RT enzyme such as zidovudine (AZT) are known treatments of HIV infection, however, these compounds have been found to inhibit other enzymes involved in DNA synthesis, leading to toxicological effects.

Attempts to circumvent toxicological disadvantages inherent in many nucleoside inhibitors such as AZT have led to the discovery of the pyrido (2,3-b) (1,4) benzodiazepinone family of compounds. One compound in particular, 5,11-dihydro-11-ethyl-5-methyl-8-(2-(1-oxido-4-quinolinyl)ethyl-6H-dipyrido(3,2-B:2′,3′-E)(1,4)diazepin-6-one (compound 1), depicted in Fig. 1, was found to be a good non-nucleoside HIV-1 reverse transcriptase inhibitor. Hence this compound became attractive as a drug development candidate with potential to be dispensed as a solid [1,2].

Because different phases of a compound can have different physical properties (e.g. density, melting point and solubility) which may lead to differences in bioavailability, process ability, and physical/chemical stability, the preparation and characterization of a compound in solid form becomes critical in the development of a drug product. To address this issue different phases of compound 1 were prepared and their physical properties were studied.

The initial preparation of compound 1 resulted in a trihydrate phase which was found to be poorly crystalline and possessed physical properties that rendered it less desirable as a drug product. The dihydrate of compound 1 was subsequently prepared which exhibited favorable thermodynamic and kinetic properties at temperature and humidity conditions used in the storage of drug products. In addition two anhydrous polymorphs, Form I and Form III were prepared having physical properties comparable to the dihydrate.

The promising properties of the dihydrate and anhydrous polymorphs (Form I and Form III) prompted extensive physical

* Corresponding author at: Boehringer Ingelheim Pharmaceuticals Inc., Analytical Sciences, 900 Ridgebury Rd., Ridgefield, CT 06877, United States.
Tel.: +1 203 798 5518.
E-mail address: nina.gonnella@boehringer-ingelheim.com (N.C. Gonnella).
[1] Current address: Genentech Inc., 1 DNA Way, South San Francisco, CA 94080, United States.
[2] Current address: Wyeth Pharmaceuticals, 401 N. Middletown Road, Pearl River, NY 10965, United States.

0731-7085/$ – see front matter © 2009 Elsevier B.V. All rights reserved.
doi:10.1016/j.jpba.2009.11.012

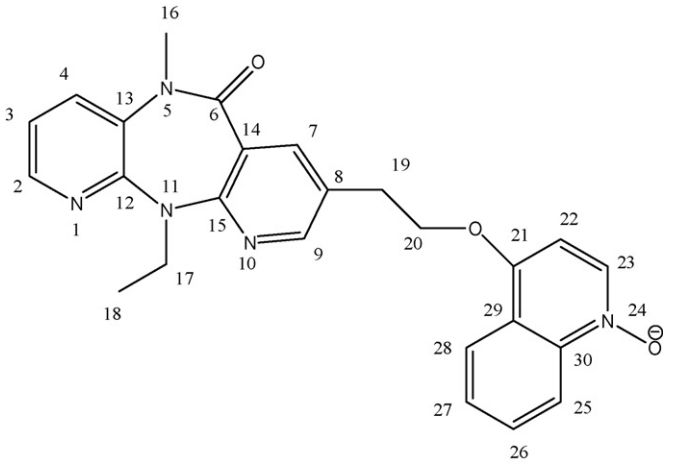

Fig. 1. Chemical structure of 5,11-dihydro-11-ethyl-5-methyl-8-(2-(1-oxido-4-quinolinyl)ethyl-6H-dipyrido(3,2-B:2′,3′-E)(1,4)diazepin-6-one (compound 1) with atom numbering.

characterization of these phases. Initial studies involved using X-ray powder diffraction (XRPD) to characterize the individual phases [3]. While this technology readily identifies the existence of various polymorph forms and hydrates, accurate measurement of low-level impurities may be difficult.

Here we report the application of ^{13}C solid-state NMR spectroscopy to study structural characteristics of compound 1 prepared as a dihydrate, and two anhydrous polymorphs (Form I and Form III). The NMR data allowed distinction among the different compound phases as well as detection of the presence of low-level impurities. Using ssNMR spectra, the relative concentrations of mixtures of the various phases could be determined from weight/percent calculations of known mixtures and integrated peak intensities. In addition, chemical shift assignments from ^{1}H and ^{13}C solution NMR studies were used in conjunction with ^{13}C ssNMR spectral editing techniques to enable full assignment of the ^{13}C ssNMR spectrum of the dihydrate. The assignments of specific carbon atoms in the molecule allowed the determination of the number of molecules in a unit cell which provides valuable information in solving the single crystal structure. Finally, insight into the relative crystallinity was determined based on ^{1}H spin-lattice (T_1) relaxation measurements. The relaxation data provides important information that may be used in the identification of compound lots having the desired physical properties.

2. Experimental

2.1. Solution NMR

Solution NMR spectra were acquired using a Bruker Avance III 600 MHz NMR spectrometer (Bruker-Biospin) operating at 600.30 MHz for ^{1}H and 150.96 MHz for ^{13}C.

Samples were dissolved in deuterated dimethylsulfoxide (DMSOd_6) and acquired with a sweep width of 8680 Hz, for proton and 36 kHz for carbon. Full ^{1}H assignments were made using COSY and NOESY experiments and full ^{13}C assignments were made from HMQC and HMBC experiments [4–7]. Proton and carbon chemical shifts were referenced to the DMSOd_6 signals at 2.5 and 39.5 ppm, respectively.

2.2. Solid-state ^{13}C NMR

Solid-state ^{13}C NMR spectra were acquired using a Bruker Avance III 400 MHz wide bore NMR spectrometer (Bruker-Biospin) operating at 100.71 MHz for ^{13}C. A Bruker H/X CP-MAS probe equipped with a 4 mm rotor was used to acquire all spectra.

Samples were packed into 4 mm zirconia rotors and sealed with Kel-F caps. Spectra were acquired using variable amplitude cross-polarization [8–11], magic angle spinning (MAS) [12,13] and high power proton decoupling with two-phase pulse modulation (TPPM) [14–17]. Contact times of 2 ms were used to acquire all spectra. The MAS frequency was 12 kHz and the proton decoupling field was approximately 49 kHz. Recycle delays, based upon saturation of ^{13}C signal intensity, were sufficiently long to allow full relaxation of ^{13}C signal. All data were collected at ambient temperature. Carbon-13 chemical shifts were quoted with respect to the external reference of adamantane (38.61 ppm).

The CPPI spectral editing techniques were employed to identify resonances corresponding to C, CH, CH_2 and CH_3 groups [18–20]. These editing techniques rely on dipolar coupling of nuclei to differentiate between the multiplicity of the carbon atoms.

The ^{13}C detected ^{1}H T_1 relaxation times were measured using a combination of a cross-polarization and saturation recovery pulse sequence [21,22]. Using Bruker Topspin software, plots of integrated signal intensity versus saturation recovery time were fit using function uxnmrt1 $[I[\tau] = I[0] + P \times \exp(-\tau/T_1)]$ where I is the integrated signal intensity, τ is the saturation recovery time and T_1 is the spin-lattice relaxation time. The best fit was calculated by varying I [0], P and T_1 in an iterative process according to the Levenberg–Marquardt algorithm. Saturation recovery times were arrayed from 100 ms to 60 s depending on the nature of the sample. A relaxation delay of 30 s was used. Integrated intensities were obtained from CP/MAS spectra using a 60 s recovery time to allow nuclei to fully relax.

3. Results and discussion

3.1. Chemical shift assignments

Solution NMR spectra, both ^{1}H and ^{13}C, were collected for compound 1 and full assignments were made that were consistent with the structure of the compound. Proton assignments were obtained using a combination of two-dimensional COSY spectra that rely on through-bond magnetization transfers as well as two-dimensional NOESY spectra that rely on through-space magnetization transfers. Integrals obtained from the 1D proton spectra were used to determine the approximate number of protons that were consistent with the structure. The COSY spectra were used to identify coupled spin systems in the molecule and to identify spins that were adjacent within a given spin system. A NOESY spectrum was used to connect spatially adjacent, non-coupled spin systems.

The ^{13}C NMR chemical shifts (δ) (referenced to dimethylsulfoxide-d_6 at 39.5 ppm) were also assigned and are consistent with the structure of compound 1. All carbon assignments were obtained using a combination of two-dimensional spectra that rely on through-bond heteronuclear magnetization transfers to delineate direct ^{1}H–^{13}C correlations (e.g. HMQC), and indirect ^{1}H–^{13}C correlations (e.g. HMBC). HMQC spectra were used to identify carbon atoms corresponding to CH, CH_2 or CH_3 groups. These assignments were verified using indirect H–C–C and H–C–C–C correlations obtained from HMBC spectra. Quaternary carbons and carbonyl carbons were assigned using pertinent HMBC cross-peaks. All cross-peaks in the HMBC spectra were consistent with the proposed assignments. The solution assignment results are shown in Table 1.

Solid-state ^{13}C NMR spectra, both CP-MAS and CPPI, were collected for the dihydrate and both anhydrous polymorphic forms of compound 1. CPPI spectra provided information on the multiplicity of the carbon resonances. This enabled each carbon to be identified as CH_3/C, CH, or CH_2. Chemical shifts were used to identify aliphatic,

Table 1
Solution and solid-state NMR assignments of compound 1.

Atom number[a]	^{1}H solution NMR δ (ppm)[b]	^{1}H solution NMR multiplicity (integral)[c]	^{13}C solution NMR δ (ppm)[b]	^{13}C solid-state NMR dihydrate δ (ppm)	^{13}C solid-state NMR Form I δ (ppm)	^{13}C solid-state NMR Form III δ (ppm)
2	8.18	dd (1)	144.03	145.5	146.3	141.3[d]
3	7.23	dd (1)	120.25	120.5[d]	119.3[d]	118.2[d]
4	7.81	m (1)	131.7	134.0	130.0[d]	131.4
6			166.27	168.0	166.9	167.5
7	8.10	m (1)	141.23	141.0	143.5	141.3[d]
8			128.87	127.9	131.0[d]	128.3
9	8.48	s (1)	151.15	154.4[d]	153.9	154.3
12			153.95	154.4[d]	155.7	153.7
13			131.12	131.6[d]	131.0[d]	131.1
14			120.28	120.5[d]	120.8[d]	118.2[d]
15			157.69	157.4	157.9	157.4
16	3.43	s (3)	36.73	39.2	37.0	39.6
17	4.06	bq (2)	40.38	43.9	41.9	47.4
18	1.12	t (3)	13.4	14.3	14.2	16.4
19	3.18	bt (2)	30.61	32.5	30.4	31.9
20	4.41	bt (2)	68.88	67.6	68.2	68.5
21			151.35	153.4	150.9	151.6
22	6.96	d (1)	101.9	100.5	98.4	100.5
23	8.43	d (1)	135.39	136.5	137.8	137.0
25	8.49	d (1)	119.24	119.3	119.3[d]	116.7
26	7.81	m (1)	130.58	131.6[d]	130.0[d]	128.9[d]
27	7.67	m (1)	128.01	125.9	128.4	128.9[d]
28	8.11	m (1)	122.28	122.0	125.8	123.4
29			122.06	120.5[d]	123.0	122.5
30			140.47	139.7	142.0	141.0

[a] For atom numbering refer to Fig. 1.
[b] Spectra acquired in DMSOd_6. ^{1}H and ^{13}C chemical shifts referenced to dimethylsulfoxide-d_6 at 2.5 and 39.5 ppm, respectively.
[c] s = singlet, dd = doublet of doublets, t = triplet, bt = broad triplet, bq = broad quartet, and m = multiplet.
[d] Resonance assignment ambiguity due to line broadening and severe overlap.

aromatic and carbonyl carbons. Assignments were also aided by the chemical shifts of carbons adjacent to heteroatoms. Because many of the carbons were well resolved, correlation with the solution spectra could be easily made. For example, resonances C20 and C22 showed distinct chemical shifts in all three forms that were specific to singular carbon atoms and upon inspection could easily be unambiguously assigned in the solid spectrum. These assignments were corroborated by the CPPI experiment which nulled C22 and inverted C20, consistent with CH and CH_2, respectively. Often areas of severe line broadening and peak overlap could be resolved using spectral editing techniques such as CPPI. For example the overlap between resonances C9 and C12 in the dihydrate could be distinguished using the spectral editing experiment where the methine C9 resonance is nulled and only the quaternary C12 remains. Comparison of the ^{13}C solution spectrum with the solid-state NMR for the dihydrate is shown in Fig. 2. Overall the correlation with the edited spectra and the solution NMR spectra showed consistent chemical shift patterns and carbon multiplicities which enabled

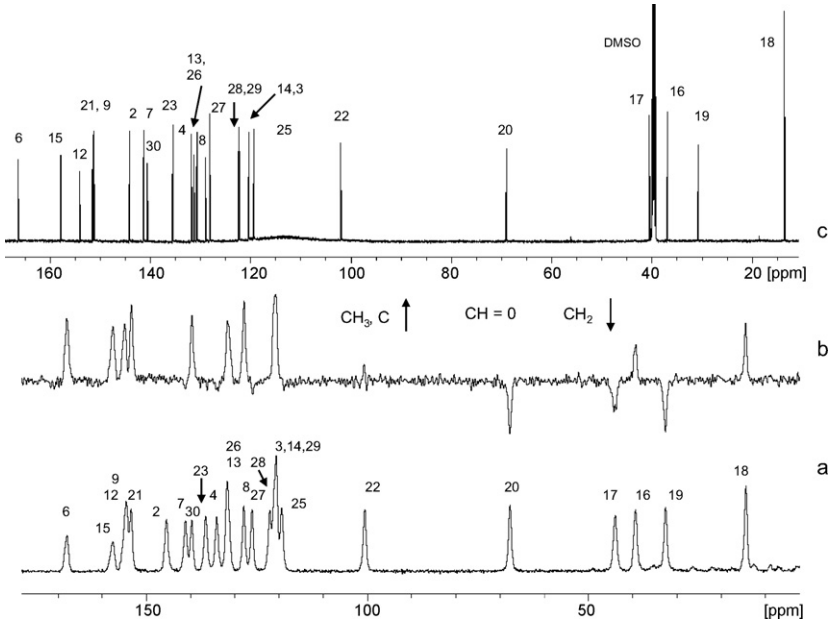

Fig. 2. (a) ^{13}C ssNMR CP/MAS spectrum of compound 1; the numbers correspond to the carbon assignments. (b) ^{13}C ssNMR CPPI spectrum of compound 1; methyl and quaternary carbons are phased up, methylene carbons are phased down and methine carbons are nulled. (c) Solution ^{13}C NMR spectrum of compound 1 in DMSOd_6; assignments were based upon 1H COSY, NOESY, HMBC and HMQC data.

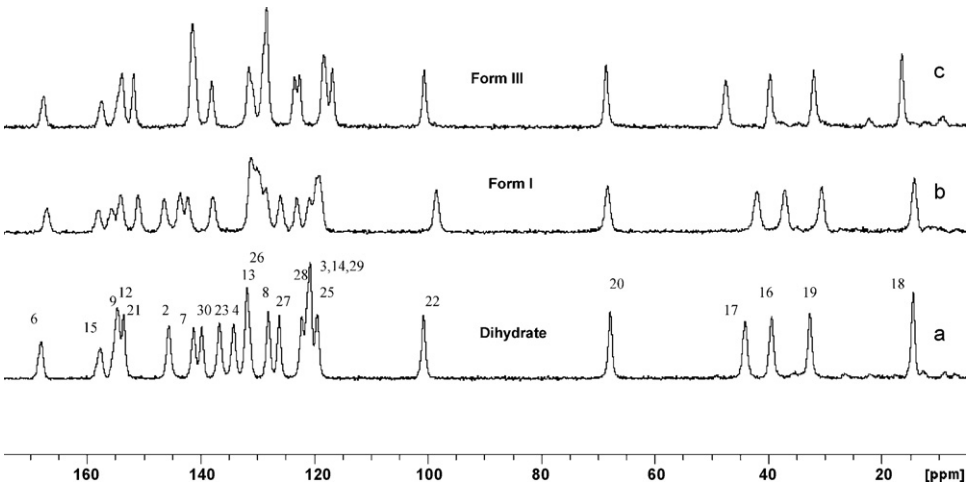

Fig. 3. ^{13}C ssNMR spectra of compound 1 show distinct chemical shift differences for the three different phases. (a) ^{13}C ssNMR spectrum dihydrate with ^{13}C chemical shift assignments shown. (b) ^{13}C ssNMR spectrum of anhydrous Form I. (c) ^{13}C ssNMR spectrum of anhydrous Form III.

unambiguous assignments to be made for the isolated spins in all three phases. However, some carbons, for example C3 and C25 in Form I, could not be unambiguously assigned due to severe overlap and common multiplicity and have been identified accordingly. The solid-state ^{13}C chemical shift assignments for all three phases are listed in Table 1.

The ^{13}C spectra acquired for polymorphs Form III and Form I showed distinct ^{13}C resonance shifts from each other and distinct differences when each form was compared with the dihydrate. The change in chemical shift patterns allowed the identities of the various phases to be easily obtained from the 1D carbon spectrum (Fig. 3). Likewise X-ray data yielded different diffraction patterns consistent with three distinct phases (Fig. 4). Hence both ssNMR spectra and XRPD data provided corroborating data for the identification of the various phases in the pure state or as mixtures.

Unlike XRPD patterns, the ssNMR spectra of the various phases of compound 1 also provided unambiguous information on the number of molecules in the asymmetric unit cell of the crystalline material. Because of our ability to make assignments at the atomic level for the resolved carbon atoms it was possible to determine that only one resonance appears for each carbon which supports the orientation of one molecule per unit cell. Isolated resonances for carbons 6, 16, 17, 18, 19, 20 and 22 (Fig. 3) are indicative of this condition. If more than one chemically equivalent molecule were present in the unit cell, multiple signals would be expected for each carbon. Hence the NMR data was consistent with one molecule per asymmetric unit for all forms studied. This particular information can be of significant value to crystallographers in structure determination studies.

3.2. Rapid quantitation of mixtures

Examination of the ^{13}C ssNMR spectrum of a sample of Form I showed the presence of an impurity. This impurity was immediately discernable as the dihydrate based upon the identical chemical shift pattern with the spectrum of the pure dihydrate and the fact that the signal intensity was a fraction of that observed for Form I (Fig. 5). Because of the chemical shift separation between the two C22 carbon resonances at ~100.49 ppm, it was possible to obtain the relative percentage of each species

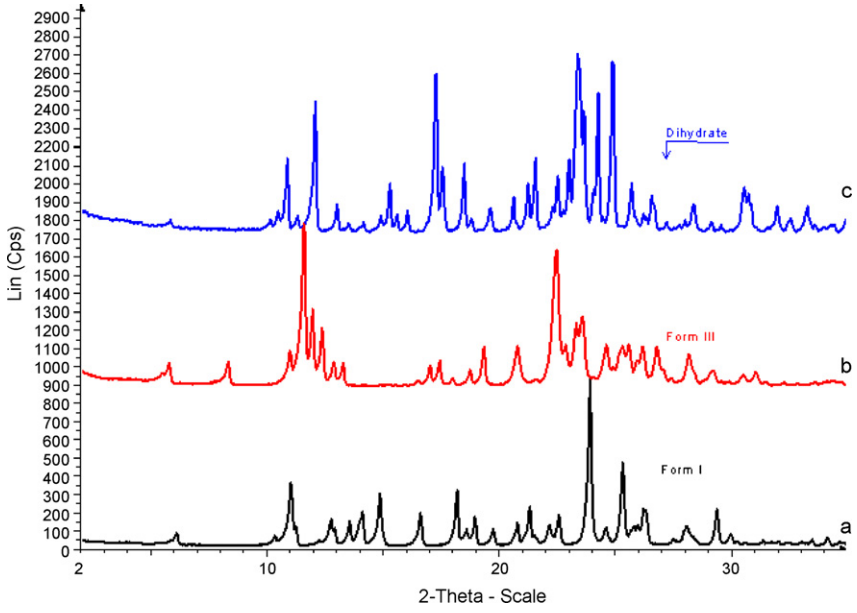

Fig. 4. X-ray powder diffraction patterns of the three phases. (a) Anhydrous Form I, (b) anhydrous Form III and (c) dihydrate.

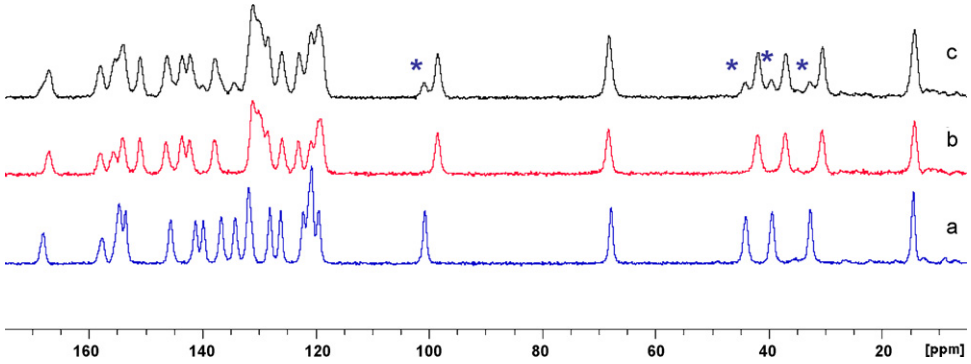

Fig. 5. ^{13}C ssNMR CP/MAS spectrum of pure phases and a mixture. (a) ^{13}C ssNMR spectrum of the pure dihydrate phase. (b) ^{13}C ssNMR spectrum of the pure anhydrous polymorph Form I. (c) ^{13}C ssNMR spectrum of the anhydrous Form I and dihydrate mixture. Peaks corresponding to the minor dihydrate component are shown with an asterisk.

using peak integration and molecular weight and without the need for deconvolution. To ensure that the integrated intensities were not compromised by differences in T_1 relaxation, ^{1}H spin-lattice relaxation data was acquired for each sample. The proton T_1 data showed the longest T_1 to be about 10.9 s. A 60 s delay was used in the collection of data to ensure full relaxation of the carbon nuclei so that the integrated peak intensities would not be affected by differences in spin-lattice relaxation. The formula used to calculate the percent composition was as follows:

$$\%\, C_A = \frac{\mathrm{Mwt_A} \times \mathrm{Int_A}}{\mathrm{Mwt_A} \times \mathrm{Int_A} + \mathrm{Mwt_B} \times \mathrm{Int_B}} \times 100\%, \quad (1)$$

where $\mathrm{Mwt_A}$ is the molecular weight of compound A; $\mathrm{Mwt_B}$ is the molecular weight of compound B; $\mathrm{Int_A}$ is the integral of a single carbon atom in compound A; $\mathrm{Int_B}$ is the integral of a single carbon atom in compound B and $\%\, C_A$ is the percent composition of compound A.

Integrated intensities of Form I showed the presence by weight of about 15% of the dihydrate and about 85% of Form I (Fig. 6a). To address the possibility that cross-polarization effects may compromise the measured peak areas, an approximate 50:50 mixture (by weight) of Form I containing the dihydrate impurity (50.1 mg) with the pure dihydrate (49.9 mg) was prepared and spectra of the mixture were acquired. The integrated intensities along with the weighed amount and the molecular weight were used to determine the weight-percent of the mixture. These results gave rise to a 58% weight composition for the dihydrate and 42% for Form I with a dihydrate/Form I molar ratio of 1.3/1 (Fig. 6b). Hence mixing the compounds gave the relative amounts in integrated intensity that would be expected based upon the weight of the two samples. It should be noted that a more rigorous ssNMR quantification involves the generation of calibration plots to correct for possible cross-polarization effects that may exist. This method has the advantage that it does not require a pure standard [23].

The presence of the dihydrate impurity in Form I was also observed in the XRPD data (Fig. 7). Similar quantitation of the dihydrate impurity in Form I could be carried out using XRPD without the need for calibration curves but XRPD requires a pure sample for the component being measured. In addition care in sample preparation needs to be controlled to prevent orientation effects from influencing the relative intensity of the diffraction lines [24] which is not required for the NMR study.

3.3. Degree of crystallinity

Both ssNMR and X-ray diffraction technologies can readily distinguish between polymorphic forms or phases. For X-ray powder diffraction, detection of the presence of crystalline defects or lower degrees of crystallinity is possible but requires the use of proper instrumentation that may not be readily available. Recently it was reported that ^{1}H T_1 relaxation data in ssNMR may be used to

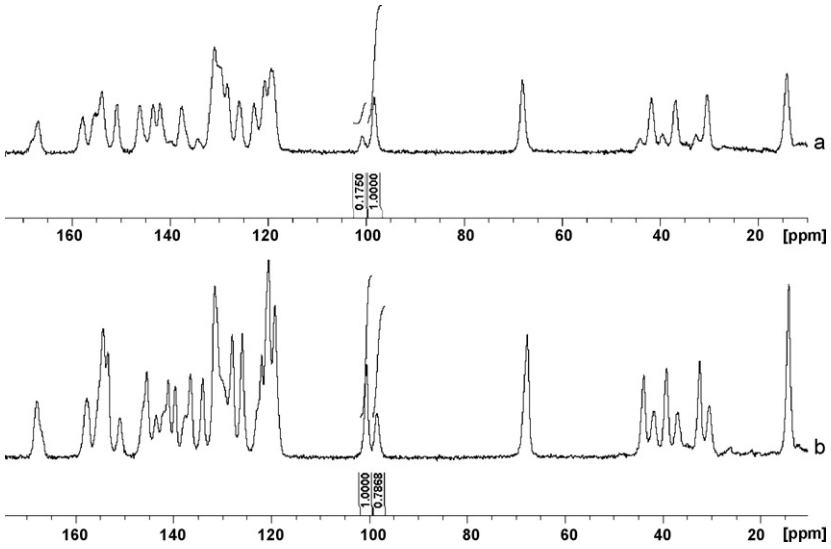

Fig. 6. (a) ^{13}C ssNMR CP/MAS spectrum of Form I with dihydrate impurity. The integrated intensities of C-22 are displayed. (b) ^{13}C ssNMR CP/MAS spectrum of ~50:50 mixture by weight Form I with dihydrate impurity and pure dihydrate. The integrated intensities of C-22 are displayed.

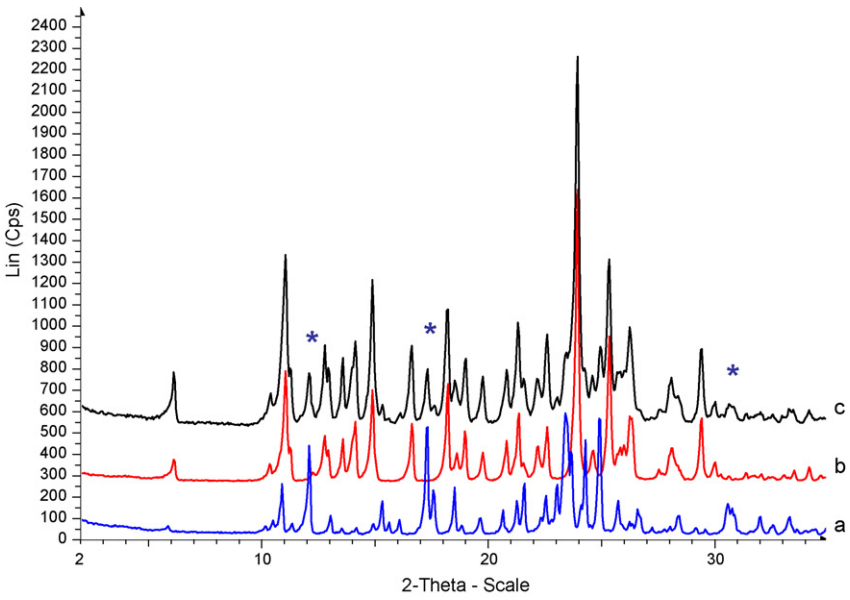

Fig. 7. X-ray powder diffraction patterns of pure phases and a mixture. (a) X-ray powder diffraction pattern of the pure dihydrate phase. (b) X-ray powder diffraction patterns of pure anhydrous polymorph Form I. (c) X-ray powder diffraction patterns of the anhydrous Form I and dihydrate mixture. Distinct peaks corresponding to the minor dihydrate component are shown with an asterisk.

determine the relative mobility of a solid phase which could provide insight into the crystalline mobility or integrity of particular pharmaceutical formulations [25]. Proton T_1 relaxation measurements in ssNMR have been found to differ significantly for different phases. Even in cases where the identical phase is examined, differences in ^{1}H T_1 relaxation data can be observed. Reasons for differences in T_1 relaxation invoke the degree of mobility at the atomic level. Possible reasons for increased mobility may be due to the incorporation of solvent in the structure or the presence of rotating methyl groups, both of which can reduce the rigid nature of the crystal lattice. In addition amorphous content or crystal defects may act as relaxation sinks to efficiently reduce T_1 through a spin diffusion mechanism. There is even evidence to suggest that particle size may affect the relaxation times by increasing the spin diffusion surface area [25]. Such conditions can impact the energy state of the solid leading to differences in the compound's physical properties. Hence it has been proposed that ssNMR ^{1}H T_1 relaxation studies may potentially be used to predict stability in the preparation of a particular solid phase [25].

In our studies with compound 1, proton T_1 relaxation data were acquired for all three phases. Representative T_1 values for selected resonances are given in Table 2. For the case of Form III, two samples (lot 1 and lot 2) prepared from the dihydrate and using the same crystallization procedure were examined. Lot 2, however, was subjected to a hammer milling process whereas lot 1 was not. As may be expected concomitant particle sizes for the unmilled lot 1 were found to be larger than for the milled lot 2, with values of approximately 60 and 25 μm, respectively. The ^{13}C ssNMR spectra of the different lot preparations of Form III showed identical ssNMR chemical shift patterns and XRPD patterns consistent with a single polymorph however, the proton T_1 relaxation times showed about a 3 s difference, with one processed lot (lot 2) relaxing about twice as fast as the other (lot 1). These differences in relaxation suggest an increase in the number of sites of mobility for lot 2 over lot 1. A possible reason for this observed phenomenon may be due to the introduction of small crystal defect sites in the milled lot which create fast relaxing domains. The effects of such domains have been reported to span distances up to 200 nm thereby contributing to the bulk relaxation in crystalline materials [25]. Another possible source for the faster relaxation would be the presence of amorphous content. Although the ^{13}C ssNMR spectra do not show evidence of detectable amorphous content for lot 2, this cannot be ruled out as a contributing factor.

Examination of the XRPD pattern of Form III (lot 2) showed an overall reduction in the signal intensity along with line broadening relative to the diffraction pattern for lot 1. Like the proton T_1 data, this XRPD result was consistent with the presence of crystal defects or amorphous content in lot 2. Hence both X-ray diffraction experiments and ^{1}H T_1 relaxation data support a lesser degree of crystallinity for lot 2. These results suggest that significant differences in T_1 relaxation for two lots of a single polymorph can provide an early approximation of the overall degree of crystallinity which can impact the physical properties of a sample.

Solid-state NMR relaxation data were also collected for the dihydrate and Form I. The relative comparison of ^{1}H T_1 measurements for the dihydrate and the three polymorph samples was as follows:

$$\text{Form I} > \text{Form III(lot 1)} > \text{Dihydrate} > \text{Form III(lot 2)}.$$

The results showed that Form I and Form III (lot 1) possessed longer ^{1}H T_1s than were observed for the dihydrate, however, comparisons of different phases are problematic due to the number of variables influencing relaxation. Longer relaxation times may be indicative of less mobility inherent in the crystal phase or could be caused by a highly structured and extensive crystalline lattice devoid of defect sites that would produce a more efficient relaxation pathway. Hence, the dihydrate relaxation properties may

Table 2
^{1}H T_1 relaxation measurements of compound 1 in the solid state.

Compound	Proton relaxation times[a,b]					
	T_{1H} (16)	T_{1H} (17)	T_{1H} (18)	T_{1H} (19)	T_{1H} (20)	T_{1H} (22)
Dihydrate	7.04	6.71	6.65	7.15	6.98	6.90
Form I[c]	10.47	10.29	10.33	10.67	9.78	8.27
Form III (lot 1)	8.61	8.67	7.74	8.26	7.87	8.07
Form III (lot 2)	5.73	4.13	4.98	4.83	5.70	4.64

[a] T_1 values are displayed in seconds.
[b] For atom numbering refer to Fig. 1.
[c] Sample contained dihydrate impurity.

suggest that the introduction of water produces a less rigid lattice and allows for more efficient spin relaxation and shorter T_1 values relative to the anhydrous polymorphs. Alternatively it is possible that water could introduce less mobility through the formation of a rigid hydrogen bonding network and other factors such as degree of crystallinity or presence of amorphous content could introduce more efficient relaxation. Based upon these considerations it would appear that relaxation studies are most relevant when comparing compound batches for a single phase. The thermal stability trend found in the melting point data showed Form I (200 °C) to be slightly greater than Form III (198 °C) which is consistent with stronger intermolecular interactions for Form 1 and correlates with the observed longer T_1 value. The dihydrate is more complicated in that it looses water starting at ~71 °C, to become a dehydrated phase which melts at ~157 °C.

Solubility experiments on these phases in an ethanol/water solvent mixture, found Form III (lot 1) to be thermodynamically preferred over pure Form I and both anhydrous forms were significantly favored over the dihydrate at 25 °C with water content below 2.7%. As water content rose above 2.7% at 25 °C, the solubility experiments showed the dihydrate to be the thermodynamically favored phase over both anhydrous polymorphs [3].

Although comparison of T_1 measurements for the anhydrous polymorphs (Form I and Form III (lot 1)) relative to the dihydrate showed agreement with solubility studies under relatively anhydrous conditions and with negligible temperature effects, comparison of T_1s for Form III (lot 1) and Form I did not correlate with solubility data where longer T_1s would be expected for Form III over Form I. Even considering the fact that the T_1 results for Form I were obtained using a mixture with 15% dihydrate present, one would expect that the dihydrate impurity would introduce an overall reduction in relaxation causing T_1s to be even longer for pure Form I. Since solubility studies showed Form III having a consistently lower solubility than Form I, the T_1 data does not appear to provide a reliable prediction of the thermodynamically preferred phase. Hence these data suggest that T_1 measurements are not predictive of dissolution phase stability when comparing different phases or phase mixtures.

4. Conclusion

Solid-state NMR has proven to be an essential source of new and corroborating information relative to X-ray powder diffraction data and is actively used to support the characterization of development candidates. Combined with solution NMR and spectral editing techniques, chemical shift assignments are possible which define a particular molecule in its solid-state environment and enable the number of molecules per asymmetric unit cell to be determined.

Mixtures of multiple forms can be readily detected based upon chemical shift patterns and relaxation measurements. This allows chemical shift patterns to be used to monitor chemical stability and phase transitions on the same sample over time. In addition, when one component in pure form is available, rapid quantitation of mixtures can be obtained from fully relaxed spectra based upon weight-percent mixtures with the pure form.

Finally, proton T_1 relaxation data provides information on structural mobility and crystallinity which impact the physical properties of the sample. While relaxation data cannot be used as a predictor of compound solubility for different phases, this information can be highly valuable in helping to evaluate transformational phase stability and in assessing the structural integrity of batch lots.

References

[1] K.D. Hargrave, J.J.R. Proudfoot, K.G. Grozinger, E. Cullen, S.R. Kapadia, U.R. Patel, V.U. Fuchs, S.C. Mauldin, J. Vitous, M.L. Behnke, J.M. Klunder, K. Pal, J.W. Skiles, D.W. McNeil, J.M. Rose, G.C. Chow, M.T. Skoog, J.C. WU, G. Schmidt, W.W. Engel, W.G. Eberlein, T.D. Saboe, S.J. Campbell, A.S. Rosenthal, J. Adams, Novel non-nucleoside inhibitors of HIV-1 reverse transcriptase. 1. Tricyclic pyridobenzo- and dipyridodiazepinones, J. Med. Chem. 34 (1991) 2231–2241.

[2] C.A. Busacca, M. Cerreta, Y. Dong, M.C. Eriksson, V. Farina, X.W. Feng, J.Y. Kim, J.C. Lorenz, M. Sarvestani, R. Simpson, R. Varsolona, J. Vitous, S.J. Campbell, M.S. Davis, P.J. Jones, D. Norwood, F. Qiu, P.L. Beaulieu, J.S. Duceppe, B. Hache, J. Brong, F.T. Chiu, T. Curtis, J. Kelley, Y.S. Lo, T.H. Powner, Development of a pilot-plant process for a nevirapine analogue HIV NNRT inhibitor, Org. Process Res. Dev. 12 (2008) 603–613.

[3] C.A. Busacca, M. Cerreta, R. Varsolona, J. Smoliga, J. Lorenz, J. Vitous, "Crystalline forms of 5,11-dihydro-11-ethyl-5 methyl-8-(2-(1-oxido-4-quinolinyl)ethyl-6H-dipyrido(3,2-B:2′,3′-E)(1,4)diazepin-6-one", US Patent No. US 7,309,700 B2, December 18, 2007.

[4] W.P. Aue, E. Bartholdi, R.R. Ernst, Two-dimensional spectroscopy. Application to nuclear magnetic resonance, J. Chem. Phys. 64 (1976) 2229–2246.

[5] A. Bax, D.G. Davis, Separation of chemical exchange and cross-relaxation effects in two-dimensional NMR spectroscopy, J. Magn. Reson. 65 (1985) 355–360.

[6] A. Bax, R.H. Griffey, B.L. Hawkins, Correlation of proton and nitrogen-15 chemical shifts by multiple quantum NMR, J. Magn. Reson. 55 (1983) 301–315.

[7] A. Bax, M.F. Summers, Proton and carbon-13 assignments from sensitivity-enhanced detection of heteronuclear multiple-bond connectivity by 2D multiple quantum NMR, J. Am. Chem. Soc. 108 (1986) 2093–2094.

[8] A. Pines, M.G. Gibby, J.S. Waugh, Proton-enhanced NMR of dilute spins in solids, J. Chem. Phys. 59 (1973) 569–590.

[9] S.R. Hartmann, E.L. Hahn, Nuclear double resonance in the rotating frame, Phys. Rev. 128 (1962) 2042–2053.

[10] A. Pines, M.G. Gibby, J.S. Waugh, Proton-enhanced nuclear induction spectroscopy. Method for high-resolution NMR of dilute spins in solids, J. Chem. Phys. 56 (1972) 1776–1777.

[11] O.B. Peersen, X. Wu, S.O. Smith, Enhancement of CP-MAS signals by variable-amplitude cross polarization. Compensation for inhomogeneous B1 fields, J. Magn. Reson. Ser. A 106 (1994) 127–131.

[12] E.R. Andrew, Narrowing of NMR spectra of solids by high-speed specimen rotation and the resolution of chemical shift and spin multiplet structures for solids, Prog. Nucl. Magn. Reson. Spectrosc. 8 (1971) 1–39.

[13] E.R. Andrew, A. Bradbury, R.G. Eades, Removal of dipolar broadening of nuclear magnetic resonance spectra of solids by specimen rotation, Nature 183 (1959) 1802–1803.

[14] J. Schaefer, E.O. Stejskal, Carbon-13 nuclear magnetic resonance of polymers spinning at the magic angle, J. Am. Chem. Soc. 98 (1976) 1031–1032.

[15] J. Schaefer, E.O. Stejskal, R. Buchdahl, High-resolution carbon-13 nuclear magnetic resonance study of some solid, glassy polymers, Macromolecules 8 (1975) 291–296.

[16] E.O. Stejskal, J. Schaefer, J.S. Waugh, Magic-angle spinning and polarization transfer in proton-enhanced NMR, J. Magn. Reson. 28 (1977) 105–112.

[17] A.E. Bennett, C.M. Rienstra, M. Auger, K.V. Lakshmi, R.G. Griffin, Heteronuclear decoupling in rotating solids, J. Chem. Phys. 103 (1995) 6951–6958.

[18] X. Wu, S.T. Burns, K.W. Zilm, Spectral editing in CPMAS NMR. Generating subspectra based on proton multiplicities, J. Magn. Reson. A 111 (1994) 29–36.

[19] X. Wu, K.W. Zilm, Methylene-only subspectrum in CPMAS NMR, J. Magn. Reson. A 104 (1998) 119–122.

[20] X. Wu, K.W. Zilm, Complete spectral editing in CPMAS NMR, J. Magn. Reson. A 102 (1993) 205–213.

[21] E.O. Stejskal, J.D. Memory, High Resolution NMR in the Solid State, Oxford University Press, New York, 1994, pp. 77–84.

[22] Peter A. Mirau, A Practical Guide to Understanding the NMR of Polymers, John Wiley & Sons, Inc., Academic Press, 2005, p. 143.

[23] T.J. Offerdahl, J.S. Salsbury, Z. Dong, D.J.W. Grant, S.A. Schroeder, I. Prkash, E.M. Gorman, D.H. Barich, E.J. Munson, Quantitation of crystalline and amorphous forms of anhydrous neotame using 13C CPMAS NMR spectroscopy, J. Pharm. Sci. 94 (2005) 2591–2605.

[24] Z. Dong, E.J. Munson, S.A. Schroeder, I. Prakash, D.J.W. Grant, Neotame anhydrate polymorphs II: quantitation and relative physical stability, Pharm. Res. 19 (2002) 1259–1264.

[25] J.W. Lubach, X. Dawei, B.E. Segmuller, E.J. Munson, Investigation of the effects of pharmaceutical processing upon solid-state NMR relaxation times and implications to solid-state formulation stability, J. Pharm. Sci. 96 (2006) 777–787.